J Mater Sci: Mater Med (2009) 20:785–792
DOI 10.1007/s10856-008-3630-z

Synthesis and characterization of Ag/Cu/HAP with platelet morphology

Hui Yang · Bingjuan Xiao · Ke-Wei Xu

Received: 28 March 2008 / Accepted: 16 October 2008 / Published online: 20 November 2008

Abstract As a useful starting material in coating technology and preparation of HAP/polymers composites the platelet Ag/Cu/HAP was prepared using the solid solution of HAP reacting with the mix-solution of silver and copper nitrate. Its composition, microstructure and properties were characterized by means of X-ray diffraction (XRD), scanning electron microscopy (SEM), Fourier transform infrared spectroscopy (FTIR) and anti-bacterial or bacteriostatic tests. The results demonstrate that the prepared Ag/Cu/HAP crystal is mainly comprised of HAP phase with little whitelockite and silver phosphate, stable up to 600°C and takes a platelet shape. At 750°C, it is partially changed into whitelockite, calcium copper phosphate, silver oxide and silver phosphate. The platelet Ag/Cu/HAP crystal has a preferential orientation of a-axis below 600°C, above which the growth in a-axis is greatly inhibited. The Ag/Cu/HAP has good crystallinity at 600°C and is the most effective powder in resisting bacteria among the HAP powders investigated. The platelet Ag/Cu/HAP crystal can be good starting materials to make antibacterial polymers/HAP composites and HAP coatings.

H. Yang · K.-W. Xu (✉)
State Key Laboratory for Mechanical Behavior of Materials, Xi'an Jiaotong University, Xi'an 710049, P.R. China
e-mail: qyh118408@163.com

H. Yang · B. Xiao
College of Life Science & Engineering, Shaanxi University of Science & Technology, Xi'an 710021, P.R. China

1 Introduction

Hydroxyapatite (HAP) is a calcium phosphate ceramic material commonly used in bone repair, both as a scaffold and as a surface coating on prosthetics. It has osteoconductive properties and a longer degradation time than other biomaterials [1]. Generally, the most popular biomaterials used as matrices for orthopedic applications are HAP composites, whereas not the pure HAP, the materials integrated with HAP including collagen type I, hyaluronic acid, the linear polymers polylactic acid (PLA) and polyglycolic acid (PGA) or copolymers of these (PLGA) [1, 2]. The problems are that these materials can hardly induce bone formation and often create an acidic environment at the implant site that leads to an inflammatory response. Other problems may be caused by implantation sites, where orthopedic patients are often susceptible to infection [3–7]. Decreased penetration of antibiotics in association with a reduced blood supply is also a significant problem. These problems can be solved by using the HAP doped with antibacterial metal ions as the biomaterials.

The transition metallic silver ion (Ag^+) and copper ion (Cu^{2+}) have stronger antibacterial properties than any other metallic ions. The antimicrobial properties of Ag^+ have been exploited for a long time in the biomedical field [8]. The significant feature of Ag^+ is its broad-spectrum antimicrobial property, which is particularly significant for the polymicrobial colonization associated with biomaterials infection [9]. The antimicrobial properties of Cu^{2+} are inferior to Ag^+, however, more effective against mold than Ag^+. The Ag^+-containing HAP (Ag/HAP) and Cu^{2+}-containing HAP(Cu/HAP) have been made and confirmed to have good antibacterial ability [10–14]. Sutter et al. [15] investigated the properties of the Cu/HAP crystal and the results show that it has a smaller dissolution rate than pure

HAP. Kim et al. [16] also synthesized the Ag/HAP, Cu/HAP powder and proved its effective antibacterial property. Therefore, the nanosized Ag/Cu/HAP may be a good biomaterial in antibacterial property and biocompatibility as it has two functional metal ions.

As mentioned above, the materials integrated with HAP include collagen type I, hyaluronic acid, PLA, PGA or PLGA in which the chemical functional group –COOH, $–NH_2$ are contained. If HAP is doped with transition metallic ions, Ag^+ and Cu^{2+}, these ions can chemically connect to –COOH, $–NH_2$ groups to form strong complex bonds according to complex theories of electronic structure [17]. Consequently, the adhesion and strength between polymers and doped HAP are enhanced.

In addition, bone is a kind of natural bioceramic composites consisting of hydroxyapatite sheets and collagen matrix [18, 19]. The hydroxyapatite sheets are of thin and long shape and parallel distribution along the orientation of the maximum main stress of the bone, which improves the maximum pullout force of the sheets and the fracture toughness of the bone. Therefore, it is necessary to prepare the platelet HAP to make the implantation of bone effectively. Many researches have been conducted to prepare the platelet HAP with great progress [20–24]. Their main focus on the preparation of the HAP coating containing platelet crystal is based on titanium substrate and the sheet HAP has no antibacterial property and can not be used to prepare the polymers/HAP composites. In this study, a platelet crystal growing mechanism is proposed and the purpose of this study was to prepare and characterize the platelet Ag/Cu/HAP with antibacterial property superior to those of the Ag/HAP and Cu/HAP and can be used as a good starting material in coating technology and to make the polymers/HAP composites.

2 Experimental

2.1 The preparation of platelet Ag/Cu/HAP crystal

Analytical grade di-ammonium hydrogen phosphate ($(NH_4)_2HPO_4$), calcium nitrate ($Ca(NO_3)_2$), silver nitrate ($AgNO_3$) and copper nitrate ($Cu(NO_3)_2$) (made in Xi'an chemicals plant) were used as starting materials to prepare the platelet Ag/Cu/HAP crystal. $(NH_4)_2HPO_4$, $Ca(NO_3)_2$ were first dissolved in the solution of nitric acid (HNO_3), and $AgNO_3$ and $Cu(NO_3)_2$ were dissolved in ammonia($NH_3 \cdot H_2O$) (made in Xi'an chemicals plant) solution. Then the solution of $AgNO_3$ and $Cu(NO_3)_2$ was dropped into that of Ca^{2+} and PO_4^{3+} to prepare platelet of antibacterial Ag/Cu/HAP crystal by stirring. The atom ratio of Ca to P in the reaction solution was set to 1.67. The slurry of Ag/Cu/HAP crystal can be formed during reaction. The obtained slurry was heated to 100°C and held for 4 h with rapid stirring, next aged for 24 h at 50°C, vacuum-filtrated, washed with deionized water and dried for 24 h at 100°C. Then the dried platelet Ag/Cu/HAP crystal was slowly cooled within the kiln to room temperature. Finally, the as-precipitated platelet of Ag/Cu/HAP samples were calcined at 300, 600, and 750°C, respectively, held for 2 h and then slowly cooled back to room temperature in the furnace. The calcining and cooling were performed in air atmosphere.

2.2 Analytical methods

The phase composition of as-precipitated Ag/Cu/HAP was analyzed by means of X-Ray diffraction (XRD) (D/max-2200PC). The operation conditions were 40 KV × 40 mA, DS-RS-SS = 1°−0.3 mm-1° by using Cu Ka. The goniometry was set at a scan rate (2θ) of 16° min^{-1} over a range (2θ) of 10° ∼ 80° and at a step size of 0.02°.

The changes of the ion groups in the Ag/Cu/HAP powder were characterized using Fourier transform infrared (FTIR) (VECTOR-22) spectroscopy. The infrared spectrum with a resolution of 4 cm^{-1} was adopted with the scan range 400–4,000 cm^{-1}. Surface morphology of the calcined Ag/Cu/HAP powder was observed by means of scanning electron microscope (SEM, JEOL 6700F). The sizes of the Ag/Cu/HAP crystal were calculated using Scherrer's equation automatically by XRD computer system.

The antibacterial property of the Ag/Cu/HAP powder dried at 100°C was tested with minimum inhibitory concentrations (MIC) method. Firstly, 0.1 g ∼ 0.2 g Ag/Cu/HAP powder was added into 100 ml liquid-casein-agar-culture by stirring and secondly, the obtained culture was diluted with the same liquid-casein-agar-culture to get various concentration cultures with the Ag/Cu/HAP powder. Then, *E. coli* and *S. mutans* ATCC 25175 were inoculated in the various obtained cultures, respectively. Next, the inoculated cultures were put into the culture box and cultured for 24 h and meantime the blank culture without any bacteria was also put into the culture box as a comparison culture. After that, the various cultures were observed and the least concentration of Ag/Cu/HAP powder with it the culture could not grow any bacteria, the same as the blank culture did, is the MIC of the Ag/Cu/HAP powder.

3 Results and discussion

3.1 The composition and stability of the platelet Ag/Cu/HAP crystal

In order to maintain the excellent bioactivity and biocompatibility of HAP crystal, the platelet Ag/Cu/HAP crystal only contains 1.5 wt% of silver and 1.5 wt% of copper, therefore, the crystal should be mainly composed of HAP phase. Figure 1 shows the XRD patterns of the

calcined Ag/Cu/HAP. Figure 2 shows XRD patterns of Ag/Cu/HAP, Ag/HAP, Cu/HAP and HAP powders calcined at 750°C. Results show that the obtained Ag/Cu/HAP crystal is mainly composed of HAP phase as mentioned above (see Fig. 1) and with slight whitelockite (TCP) and silver phosphate ($Ag_4P_2O_7$) below 600°C(see Fig. 2).

The radii [25] of Cu^{2+} and Ag^+ are 0.73 Å and 1.15 Å, respectively, close to that of Ca^{2+} (1.00 Å), and therefore, can substitute for the Ca^{2+} in the lattice of HAP leading to

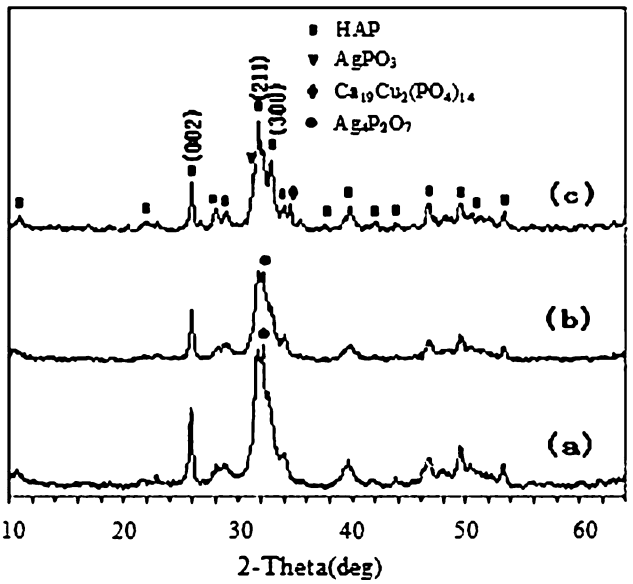

Fig. 1 XRD patterns of as-produced Ag/Cu/HAP composite sintered at **a** 100°C, **b** 300°C, **c** 600°C

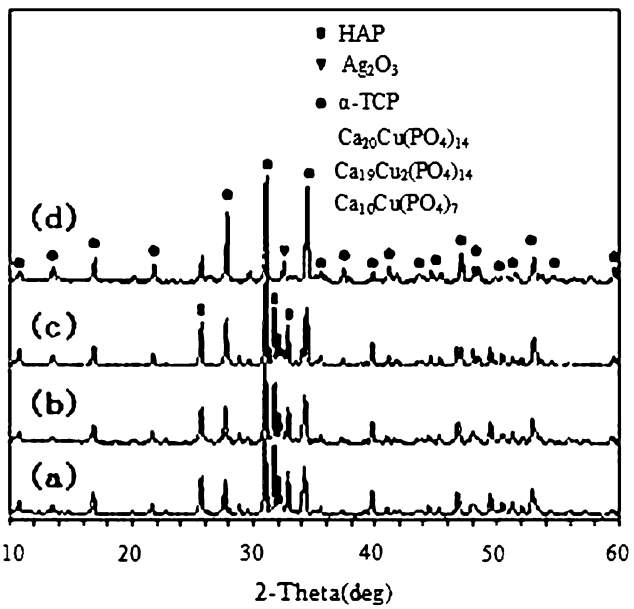

Fig. 2 XRD patterns of the powders calcined at 750°C **a** HAP, **b** Ag/HAP, **c** Cu/HAP, **d** Ag/Cu/HAP

the microstructure change of the HAP lattice, the increase of the disorder-random or entropy(S) of the lattice and the reduction of crystallinity of HAP theoretically. The obtained Ag/Cu/HAP having the broadened peaks as the Fig. 1 described indicates that it is a weak crystal. The results show that in the temperature range from 100 to 600°C, the HAP phase in the Ag/Cu/HAP was stable. At 600°C, a very small part of it reacts with copper and silver leading to form calcium copper phosphate ($Ca_{19}Cu_2(PO_4)_{14}$), implying that Cu^{2+} substituted for Ca^{2+} in HAP lattice and meantime dehydroxylation reaction occurred, the OH^- was lost and $Ag_4P_2O_7$ was changed into $AgPO_3$. At 750°C, more Ag/Cu/HAP was changed into whitelockite ($Ca_3(PO_4)_2$), calcium copper phosphate ($Ca_{20}Cu(PO_4)_{14}$, $Ca_{19}Cu_2(PO_4)_{14}$ and $Ca_{10}Cu(PO_4)_7$), silver phosphate ($AgPO_3$) and silver oxide (Ag_2O_3), which indicate that at low temperature only some of Ag^+ and Cu^{2+} with high energy could substitute the Ca^{2+} in HAP lattice, and at high temperature more energy can be provided to Ag^+ and Cu^{2+}-containing HAP and make the Ag^+ and Cu^{2+} substitute Ca^{2+} in HAP lattice to form $Ca_{19}Cu_2(PO_4)_{14}$ obviously. Figures 1 and 2 show that the obtained Ag/Cu/HAP crystal contains slight TCP and $Ag_4P_2O_7$ below 600°C which is because during the preparation of Ag/Cu/HAP crystal the ammonia solution of $AgNO_3$ and $Cu(NO_3)_2$ was dropped into the acidic solution of Ca^{2+} and PO_4^{3+}, and the circumstances of synthesis is changed from a acidic condition to a basic one. In this process PO_4^{3-} can exist in three forms, $H_2PO_4^-$, HPO_4^{2-}, PO_4^{3-} in aqueous solution, therefore, the HAP crystal or doped HAP crystal synthesized by the wet method in this study probably contain little impurity [26]. At 600°C the obtained Ag/Cu/HAP crystal is purified due to the impurity decomposition (see Fig. 1). At 750°C more TCP and calcium copper phosphates are formed and the relative intensities of HAP diffraction peaks are suddenly reduced which is similar to the observations reported by Pattanayak et al. [27]. They pointed that the HAP prepared by wet method was stable up to 600°C and the formation of major amount of TCP and other calcium phosphate were mainly caused by the dehydroxylation reaction of HAP occurred above 600°C, and with an increase in calcination temperature HAP would have started losing hydroxyl groups forming various phosphates. In a truly anhydrous system, HAP should not appear due to the dehydroxylation reaction. In this study, at 750°C an anhydrous system is basically formed (see Fig. 4), so various phosphates are formed.

Pattanayak et al. [27] crystallographically studied the XRD patterns of the end products of HAP over 600°C and confirmed that the end products seem apatitic because the diffraction maxima of the products produced in dehydroxylation overlap those of HAP and the formed TCP seem to exhibit an apatite lattice, rather than that of whitelockite, which is believed possible due to the inclusion of lattice

defects. In this study, the obtained XRD patterns at 750°C are much similar to those got by Pattanayak therefore, the end products in this study should be apatitic. Pattanayak also pointed that the reduces of the relative intensity of HAP in the XRD patterns with increase in calcinations temperature does not really indicate the absence of HA-like phases.

There are many factors affecting the thermal stability of HAP crystal. Many literatures indicated that HAP crystal should be stable up to 1,200°C or at higher temperature. For examples, Saeri [28] synthesized HAP powders with wet method using pure raw materials and degassed distilled water to prepare all the solutions and filtered inert Ar as the protective gas of the reaction system, the filter containing a sufficient amount of carbon dioxide absorber (KOH), the obtained powders could exist stably up to 1,200°C. Rapacz-Kmita [29] synthesized HAP powder using CaO and H_3PO_4 as starting materials with wet method and the obtained HAP powder was stable in a hot pressing process over 1,000°C. Kothapalli [30] prepared HAP powders using wet method with 7 days aging. The obtained HAP powders could keep stable when the powders were pressed into half-inch diameter disks at a pressure of 150 MPa for 1 min and sintered in air at 1,200°C for 1 h with a heating rate of 5°C/min. Meejoo [31] synthesized HAP powder using $Ca(OH)_2$ and $(NH_4)_2HPO_4$ as starting materials with a microwave radiation wet method and the synthesized powders were stable up to 900°C. It is reported that using $Ca(NO_3)_2 \cdot 4H_2O$, phosphoric acid (H_3PO_4), $NH_3 \cdot H_2O$ and β-glucose as starting materials, Yang [32] synthesized various HAP powders having different thermal stability with microwave irradiation method and coprecipitation method, respectively. At calcination of 1,000°C, the HAP powders obtained with different aging and irradiating time had different predominant phase, aged for 4 and 8 h are β-$Ca_3(PO_4)_2$ and CaO. HAP and a little β-$Ca_3(PO_4)_2$ were observed by aging for 12 h, and the polycrystals of HAP can exist stably by aging for 24 h. At calcination of 1,200°C, the sample completely transform to β-$Ca_3(PO_4)_2$ and CaO by aging for 12 h, and the samples aged for 24 h are still HAP. The sample irradiated for 30 min completely transforms to β-$Ca_3(PO_4)_2$ and CaO, and sample irradiated for 1 h is still HAP at 1,200°C. The power of microwave also influenced the thermal stability of the obtained HAP powders in Yang's research. Moreover, the HAP being stable above 1,000°C was also synthesized by our group with Triton-X-100/hexanol/cyclohexane inverse microemulsion system. In short, the thermal stability of HAP powders is a function of the type of starting materials, the synthesis method used, preparation condition including post-treatment after precipitation and so on. In this study, the obtained platelet Ag/Cu/HAP powders can stable up to 600°C, this is associated to the starting materials, the conditions used in wet method, the acidity changes in preparation and the dehydroxylation during the calcinations over 600°C.

3.2 Crystal size of the platelet Ag/Cu/HAP crystal

The crystal size of the Ag/Cu/HAP is an important parameter to characterize and the size change in the transformation from HAP to Ag/Cu/HAP can give some important information about the reaction during the formation of Ag/Cu/HAP. It was reported [33] that Mg^{2+}(aq) with the radius of 0.72 Å can replace Ca^{2+} with the radius of 1.00 Å in the HAP crystal and inhibit the growth of crystal, thus forming HAP crystals of small size. Cu^{2+}(0.73 Å), almost the same as Mg^{2+} in charge and size, can replace Ca^{2+} and form HAP of small size. When Ag^{+}(1.15 Å) substitutes for Ca^{2+}, HAP crystals of larger size are formed since Ag^{+} is larger in size and lower in charge than Ca^{2+}. Table 1 shows the crystal sizes of the Ag/Cu/HAP calcined at different temperatures, indicating that based on peaks (002), (300) and (211) Ag/Cu/HAP change slightly in sizes at temperatures from 100 to 750°C, except that based on peak 300 at 750°C. Based on peaks (002), (300) at the temperatures from 100 to 750°C, Ag/Cu/HAP is larger in size than Cu/HAP and smaller than HAP while it is close to Ag/HAP. Based on peak (300) the Ag/Cu/HAP has the largest sizes at 100 and 300°C and almost the smallest size at 600°C of the four kinds of HAP crystals in Table 1. This indicates that, the Ag/Cu/HAP crystal preferentially grows in the direction of a-axis below 600°C.

Table 1 The particle size of different HAP powders calcined at temperature varying from 100°C to 750°C

Sample	Temperature/°C	Particle size/nm		
		(002)	(300)	(211)
Ag/Cu/HAP	100	24.1	34.2	9.0
	300	26.0	34.7	8.7
	600	25.8	18.4	10.7
	750	/[a]	/[a]	/[a]
HAP	100	28.9	19.4	12.6
	300	26.1	17.1	12.5
	600	28.7	20.2	13.5
	750	30.6	44.1	50.7
Ag/HAP	100	26.0	17.2	11.4
	300	27.9	19.0	11.5
	600	26.9	19.8	14.5
	750	28.3	46.8	56.1
Cu/HAP	100	23.0	19.7	13.3
	300	22.0	12.7	13.9
	600	21.7	18.2	13.6
	750	35.5	35.7	21.7

[a] Without related size value as the Ag/Cu/HAP crystal was completely decomposed into α-TCP and other phosphate at 750°C

At and above 600°C, the growth in the direction of a-axis is inhibited strongly because of the polarization and extrapolarization in Ag/Cu/HAP lattice. According to the theory of ion polarization, Ag^{+} and Cu^{2+} are transition metallic ions and capable of influencing the shapes of OH^{-} and PO_4^{3-}. Furthermore, at and above 600°C, Ag^{+}, Cu^{2+} and OH^{-}, PO_4^{3-} in HAP lattice influence each other to intensify the chemical connection between them, resulting in an extra-polarization and, consequently, the lattice space becomes smaller and smaller until it reaches a thermodynamic equilibrium state. In this case the Ag/Cu/HAP has a high lattice energy or high surface free energy. As a result, the Ag/Cu/HAP tends to grow evenly in axes a, b and c. The surface area of lattice is reduced, the Ag/Cu/HAP remains stable and meantime the platelet Ag/Cu/HAP crystal has the smallest size.

3.3 The chemical action in the platelet Ag/Cu/HAP crystal

Figure 3 shows the FTIR spectra of the calcined Ag/Cu/HAP powders at various temperatures. The spectra have characteristic features of crystalline HAP with some carbonate substitution. Two bands at 603 and 570 cm^{-1} represent v_4O–P–O bending vibrations of PO_4^{3-} groups in phosphate. The peak at 962 cm^{-1} reflects the v_1P–O symmetric stretch. The bands located at 1,044 and 1,091 cm^{-1} result from v_3P–O antisymmetric stretching vibration. The band at 473 cm^{-1} belongs to v_2P–O stretching vibration (see Fig. 3). The bands at 1,411 and 1,456 cm^{-1} result from the carbonate groups incorporated in the Ag/Cu/HAP structure and the background carbon dioxide (CO_2) in the atmosphere. The bands at 3,443 and 1,630 cm^{-1} indicate water absorbed in the Ag/Cu/HAP powder (see Fig. 3). Two bands for structural OH^{-} groups at 633 and 3,570 cm^{-1} are detected and progressively enhanced as the temperature increases from 100 to 600°C.

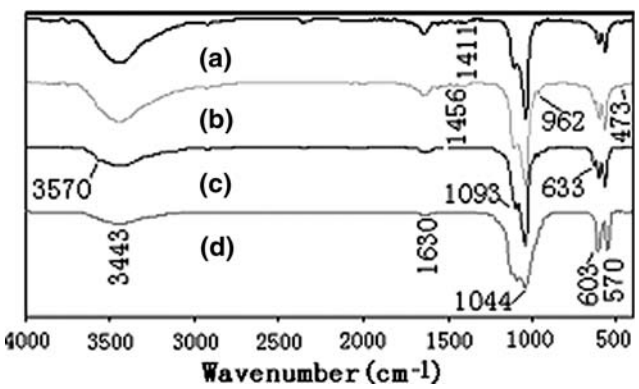

Fig. 3 FTIR spectra of the Ag/Cu/HAP powders calcined at **a** 100°C, **b** 300°C, **c** 600°C and **d** 750°C

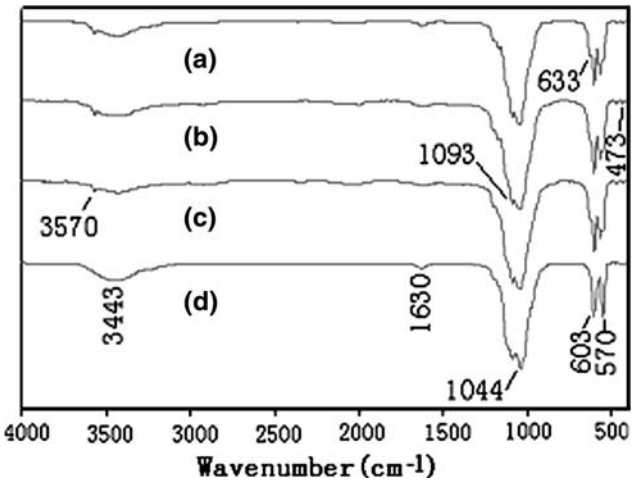

Fig. 4 FTIR spectra of **a** HAP, **b** Ag/HAP, **c** Cu/HAP, **d** Ag/Cu/HAP powders calcined at 750°C for 2 h

In fact, at 600°C the bands are significantly exposed in spectra, which indicate the Ag/Cu/HAP has good crystallinity at 600°C. At 750°C, the band located at 633 cm^{-1} for the structural OH^{-} group disappears due to the dehydroxylation of HAP, whereas the band labeled at 3,570 cm^{-1} remains a weak peak (see Fig. 4).

At low temperature the peak of OH^{-} group was blurring and at 600°C it turned obvious (see Fig. 3), fitting well to XRD analysis in 3.1, which indicates Ag^{+} and Cu^{2+} in the Ag/Cu/HAP mainly bond with OH^{-} group with none or very little, combined with the PO_4^{3-} group below 600°C. However, at high temperature they enter to the lattice of HAP and mainly bond with the PO_4^{3-} group. As a result, the Ag/Cu/HAP further is crystallized.

Figure 4 indicates the four types of HAP dehydroxylation at 750°C and the bands located at 633 cm^{-1} and 3,570 cm^{-1} for structural OH^{-} group almost disappear, well corresponding to that the Ag/Cu/HAP easily changes into $Ca_{20}Cu(PO_4)_{14}$, $Ca_{19}Cu_2(PO_4)_{14}$ and $Ca_{10}Cu(PO_4)_7$ during dehydroxylation and meantime the substitution of Ag^{+}, Cu^{2+} for Ca^{2+} in the HAP lattice occurs.

3.4 The growing mechanism of the platelet Ag/Cu/HAP crystal

According to the model of the surface structure of HAP provided by Kawaski [34], on surface *c* there is a strong absorption center known as site c and a weak absorption center of cations known as site P, and on surface *a* or *b* there are absorption centers for the anions. In this study, the start pH of the reaction solution is <4. Though the pH increases as the reaction continues, it is still <7 when the HAP is formed. In this case, a great amount of H_3O^{+} and NH_4^{+} exist in the solution of reaction and they can be

absorbed by the group of PO_4^{3-} on surface *c*. The group of PO_4^{3-} is protonated to form HPO_4^{2-} or $H_2PO_4^-$. As a result, the electric potential and the ability to absorb Ca^{2+} are reduced or inhibited on surface *c*. Further more, in the acidic environment, the OH^- located on surfaces *a* and *b* are easily missing, which causes a great amount of HPO_4^{2-} or $H_2PO_4^-$ to move to surfaces *a* and *b* and to be absorbed. Consequently, Ca^{2+} ions are absorbed and form a layer of Ca^{2+} outside that of HPO_4^{2-} or $H_2PO_4^-$, which forms a highly concentrated area of Ca^{2+}, HPO_4^{2-} or $H_2PO_4^-$. Therefore, as the reaction continues, the HAP crystal will rapidly precipitate and preferentially grow in the directions of *a*-axis and *b*-axis and forms the Ag/Cu/HAP platelets. In addition, the HPO_4^{2-} or $H_2PO_4^-$, different from OH^- in size, charges and microstructure, substitutes for the OH^- on the surfaces *a* and *b* and will change the growth tendency of the HAP crystal [35], which enhances the formation of the platelet Ag/Cu/HAP crystal.

Figure 5 shows the SEM micrographs of four kinds of HAP nanosized particles at 100°C which indicate that the morphologies of the former three nanosized HAP powders are basically needle shape with a diameter of 30 $\sim$ 80 nm and a length of 300 $\sim$ 500 nm. The Ag/Cu/HAP powder takes the platelet shape as mentioned above.

Figure 6 depicts the SEM micrographs of the platelet Ag/Cu/HAP calcined at 100, 300, 600, and 750°C and the results show that below 600°C the crystal is basically sheet-like in shape whereas at 750°C, a great change in shape occurs. In fact, it changes into a spherical shape. This corresponds well to the XRD patterns and FTIR spectra of the Ag/Cu/HAP at various temperatures (see Figs. 1–3).

3.5 Anti-bacterial test

Ag^+ and Cu^{2+} are transition metallic ions and have the ability to complex with anions such as $–NH_2$, –S–S– and –CONH– of protein or enzyme in the bacterial cells. They, therefore, can damage the DNA and RNA of bacteria or inhibit its propagation when they are released from the Ag/Cu/HAP crystal in the solution. In addition, the Ag/Cu/HAP crystal has a large surface area as it is a nanosized particle, which makes bacteria adhere to the surface of the Ag/Cu/HAP crystal. Table 2 presents the antibacterial test results of the four kinds of HAPs. The results prove that, the doped HAP powders investigated have strong antibacterial or bacteriostatic properties and the Ag/Cu/HAP powder is the strongest antibacterial agent due to the cooperation between Cu^{2+} and Ag^+ ions against bacteria whereas the pure HAP powder does not have any antibacterial property.

The cytotoxicity of the metallic ions doped HAP crystal, which is related to its antibacterial property, have attracted many peoples' attention and many researches related to this issue have been done. Oh [36] studied the cytotoxicity of Ag doped HAP through various routes and the results showed that the optimal antimicrobial property with none

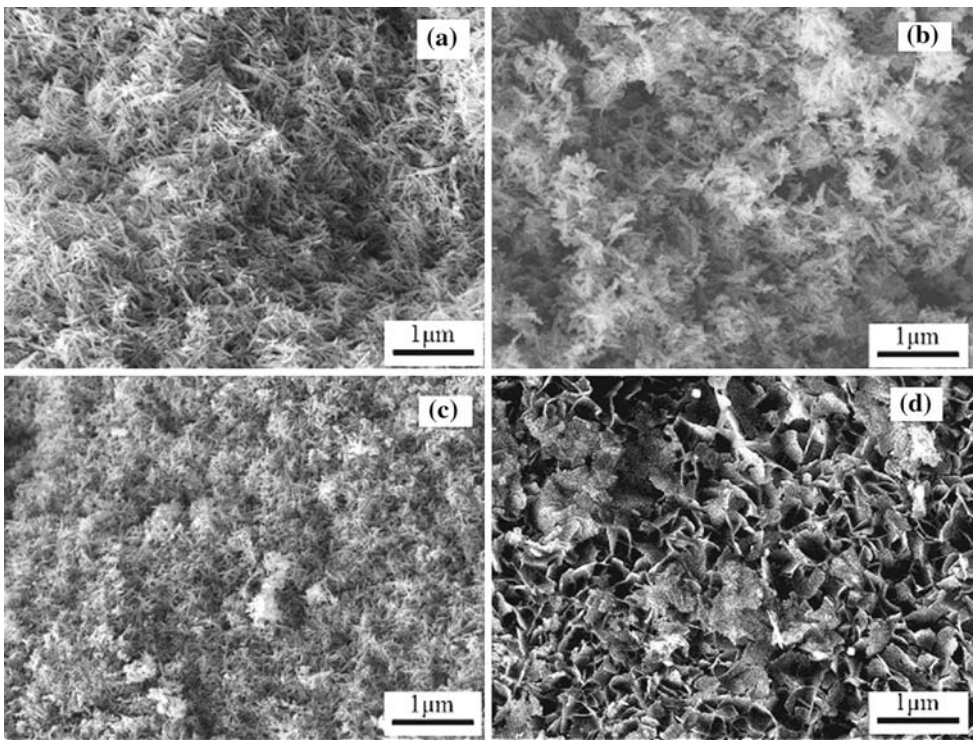

Fig. 5 The SEM micrographs calcined at 100°C of **a** HAP, **b** AgHAP, **c** CuHAP and **d** AgCuHAP

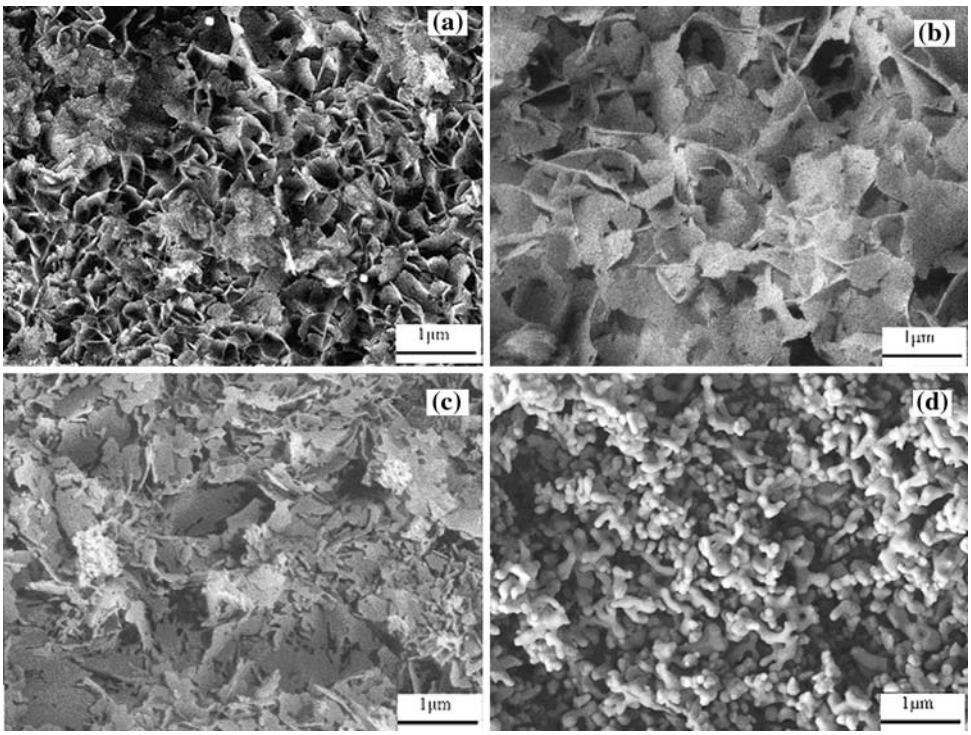

Fig. 6 The SEM micrographs of the AgCuHAP platelet calcined at **a** 100, **b** 300°C, **c** 600°C and **d** 750°C

Table 2 The minimum inhibitory concentrations (MIC) of the four HAP against *E. coli* and *S. Aureus*

Sample[a]	MIC[b]/ppm	
	Against *E. coli*	Against *S. mutans*
HAP	/	/
Ag/HAP	5	5
Cu/HAP	10	10
Ag/Cu/HAP	3.4	3.4

[a] Sample sintered or dried at 100°C for 20 h

[b] Minimum inhibitory concentrations

/: Without antibacterial property

or mild cytotoxicity may be produced by modulating not only the doped silver amount but also their shape and synthesis route. Chen [37] conducted a comparison study on the cytotoxicity between the co-sputtered silver (Ag)-containing HAP coating and pure HAP coating. The results indicated that no significant difference in the in vitro cytotoxicity was observed between HA and Ag-HA surfaces. Verne [38] characterized the Ag doped bioactive glass by means of SEM observation, EDS analysis, bioactivity test (soaking in a simulated body fluid), leaching test (GFAAS analyses) and cytotoxicity test. It is demonstrated that these surface silver-doped glasses maintain, or even improve, the bioactivity of the starting glass. The measured quantity of released Ag into simulated body fluid compares those reported in literatures for the antibacterial activity and the non-cytotoxic effect of Ag. Catauro [39] also investigated the bioactivity of Ag doped bioactive glass and reported that the FTIR measurements and SEM micrographs had ascertained the formation of a hydroxyapatite layer on the surface of samples soaked in a simulated body fluid for different times. Cu^{2+}, as mentioned above, is inferior to Ag^{+} in terms of antibacterial property. Sutter's [15] research results showed that the Cu^{2+} doped HAP has a smaller dissolution rate than pure HAP. Therefore, it can be estimated that Cu^{2+} can have none or mild cytotoxic effect to human being through modulating the doped copper amount and synthesis route. Further more, a main application of the Ag/Cu/HAP crystal is to prepare enhanced implants materials, polymers/HAP composites, in these biomaterials the cytotoxicity of Ag^{+} and Cu^{2+} will be reduced to a great extent due to the dilution of polymers and the chemical connection between them and the –COOH, $–NH_2$ groups contained in polymers. And also the thermal stability of the platelet Ag/Cu/HAP crystal up to 600°C is satisfactory because the synthesis of polymers/HAP composites will be carried out under low temperatures due to polymers' poor thermostability.

4 Conclusion

The investigated Ag/Cu/HAP crystal includes mainly HAP phase with a little whitelockite ($Ca_3(PO_4)_2$) and silver

phosphate ($Ag_4P_2O_7$) below 600°C. It is platelet and is a weak crystal that is stable at and below 600°C. At 750°C, $Ca_3(PO_4)_2$, $Ca_{20}Cu(PO_4)_{14}$, $Ca_{19}Cu_2(PO_4)_{14}$, $Ca_{10}Cu(PO_4)_7$, Ag_2O_3 and $Ag_4P_2O_7$ are formed due to the dehydroxylation reaction of HAP crystal. The platelet Ag/Cu/HAP crystal has preferential orientation of *a*-axis below 600°C, above which the growth in the direction of *a*-axis is inhibited greatly. The FTIR spectra show that Ag^+ and Cu^{2+} in the platelet Ag/Cu/HAP combine with OH^- group below 600°C, above which they are bound with PO_4^{3-} group. The platelet Ag/Cu/HAP has a good crystallinity at 600°C and is the strongest antibacterial agent among the investigated HAP powders. The platelet Ag/Cu/HAP crystal with these properties can be used as good starting materials to make the polymers/HAP composites and HAP coating.

Acknowledgments This work was financially supported by the Key Research Item of Technology of Bureau of Sci. & Technol. of Xi'an city, Shaanxi Province of China (Grant no. GG 200354) and partially supported by the Natural Science Foundation of Shaanxi Province of China (Grant No. 2004B24) and the Research Team Foundation of Shaanxi University of Sci. & Technol.(sust-B104).

References

1. J.E. Fleming, C.N. Cornell, G.F. Muschler, Orthop. Clint. North. Am. **31**, 357–374 (2000)
2. S.N. Khan, Entomic, J.M. Lane, Orthop. Clin. North. Am. **31**, 389–398 (2000)
3. C.M. Court-Brown, in *Management of Open Fractures*, ed. by Dunitz Martin (United Kingdom, 1996)
4. R.D. Inman, K.V. Gallegos, B.D. Brause, P.B. Redecha, C.L. Christian, Am. J. Med. **77**, 47–53 (1984)
5. P.J. Sanderson, J. Hosp. Infect.**18**(Suppl A), 367–375 (1991)
6. J.M. Schierholz, J. Beuth, J. Hosp. Infect. **49**, 87–93 (2001)
7. B. Sugarman, E.J. Young, Infect. Dis. Clin. North. Am. **31**, 187–198 (1989)
8. M. Bellantone, N.J. Coleman, L.L. Hench, J. Biomed. Mater. Res. **51**, 484–490 (2000)
9. A.G. Gristina, Science. **237**, 1588–1595 (1987)
10. J.J. Blaker, S.N. Nazhat, A.R. Boccaccini, Biomaterials. **25**(7–8), 1319–1329 (2004)
11. R.J. Chung, M.F. Hsieh, C.W. Huang, L.H. Perng, H.W. Wen, T.S. Chin, J. Biomed. Mater. Res—Part B: Appl. Biomater. **76**(1), 169–178 (2006)
12. R.J. Chung, M.F. Hsieh, K.C. Huang, L.H. Perng, F.I. Chou, T.S. Chin, J. Sol–Gel. Sci. Technol. **33**(2), 229–239 (2005)
13. K.S. Oh, K.J. Kim, Y.K. Jeong, Y.H. Choa, Key Eng. Mater. **240–242**, 583–586 (2003)
14. J.D. Li, Y.B. Li, Y. Zuo, G.Y. Lu, W.H. Yang, L.R. Mo, J. Funct. Mater. **37**(4), 635–638 (2006) (in Chinese)
15. B. Sutter, D.W. Ming, A. Clearfield, L.R. Hossner, J. Soil. Sci. Soc. Am. **67**(6), 1935–1942 (2003)
16. T.N. Kim, G.L. Feng, J.O. Kim, J. Wu, H. Wang, G.C. Chen, F.Z. Cui, J. Mater. Sci: Mater. Med. **9**(3), 129–134 (1998)
17. G.L. Miessler, D.A. Tarr (eds.), *Inorganic Chemistry* (Pearson Education, Inc, Upper Saddle River, New Jersey, 2004), pp. 337–376
18. B. Chen, X.H. Peng, X.Y. Wu, Key Eng. Mater. **334–335**(II), 1129–1132 (2007)
19. B. Chen, X.Y. Wu, X.H. Peng, Key Eng. Mater. **330–332**(II), 785–788 (2007)
20. B.Y. Chen, C.H. Liang, Ceram. Int. **33**(4), 701–703 (2007)
21. K. Loku, S. Yoshimura, H. Fujimori, S. Goto, M. Yoshimura, Solid State Ionics. **151**(1–4), 147–150 (2002)
22. A.C. Lawson, J.T. Czernuszka, Mater. Res. Soc. Symposium-Proceedings. **550**, 273–278 (1999)
23. J.X. Zhang, M. Maeda, N. Kotobuki, M. Hirose, H. Ohqushi, D.L. Jiang, M. Lwasa, Mater. Chem. Phys. **99**(2–3), 398–404 (2006)
24. K. Yamauchi, T. Goda, N. Takeuchi, H. Einaqa, T. Tanabe, Biomaterials. **25**(24), 5481–5489 (2004)
25. G.D. Zhou, *Inorganic Chemistry Series*. Science Press, Beijing: China **30**(11), 296–300 (1982). R.D. Shannon, Acta. Cryst. A32, 1976:751
26. J.C. Elliott, Structure and chemistry of the apatites and other calcium orthophosphates, in *Studies in Inorganic Chemistry*, ed. by J.C. Elliott (Elsevier, Amsterdam, 1994), pp. 148–154
27. D.K. Pattanayak, R.C. Rajalaxmi Dash, B.T. Prasad, T.R. Rao, Rama Mohan, Mater. Sci. Eng. C. **27**, 684–690 (2007)
28. M.R. Saeri, A. Afshar, M. Ghorbani, N. Ehsani, C.C. Sorrell, Mater. Lett. **57**, 4064–4069 (2003)
29. A. Rapacz-Kmita, C. Paluszkiewicz, A. S′ lo′sarczyk, Z. Paszkiewicz, J. Mol. Struct. **744–747**, 653–656 (2005)
30. C. Kothapalli, M. Wei, A. Vasiliev, M.T. Shaw, Acta. Mater. **52**, 5655–5663 (2004)
31. S. Meejoo, W. Maneeprakorn, P. Winotai, Thermochimica. Acta. **447**, 115–120 (2006)
32. Z.W. Yang, Y.S. Jiang, Y.J. Wang, L.Y. Ma, F.F. Li, Mater. Lett.**58**, 3586–3590 (2004)
33. N. Kanzaki, K. Onuma, G. Treboux, S. Tsutsumi, A. Ito, J. Phys. Chem. B. **104**(17), 4189–4194 (2000)
34. W. Sheng, Y.F. Gu, C.S. Liu, X.M. Sun, L.M. Hu, *Gui suan yan tong bao*, **1**:45–52 (1996) T. Kawasaki et al., J. Chromatography. 515 (1990) 125
35. W. Sheng, Y.F. Gu, C.S. Liu, X.M. Sun, L.M. Hu, Gui. Suan. Yan. Tong. Bao. **1**, 45–52 (1996)
36. K.S. Oh, K.J. Kim, Y.K. Jeong, E.K. Park, S.Y. Kim, J.H. Kwon, H.M. Ryoo, H.I. Shin, Key Eng. Mater. **264–268**, 2107–2110 (2004)
37. W. Chen, Y. Liu, H.S. Courtney, M. Bettenga, C.M. Agrawal, J.D. Bumgardner, J.L. Ong, Biomaterials. **27**, 5512–5517 (2006)
38. E. Verne, S. Di Nunzio, M. Bosetti, P. Appendino, C. Vitale Brovarone, G. Maina, M. Cannas, Biomaterials. **26**, 5111–5119 (2005)
39. M. Catauro, M.G. Raucci, F. De Gaetano, A. Marotta, J. Mater. Sci: Mater. Med. **15**(7), 831–837 (2004)